Heliyon 10 (2024) e33418

Contents lists available at ScienceDirect

Heliyon

journal homepage: www.cell.com/heliyon

Research article

Metabolomics analyses reveal the liver-protective mechanism of Wang's metabolic formula on metabolic-associated fatty liver disease

Suhong Chen [a,c,d,1], Jiahui Huang [a,d,1], Yuzhen Huang [a,d,1], Chengliang Zhou [a,d], Ning Wang [a,d], Linnan Zhang [a,d], Zehua Zhang [a,d], Bo Li [a,d], Xinglishang He [a,d], Kungen Wang [b,e,****], Yihui Zhi [b,e,***], Guiyuan Lv [c,**], Shuhua Shen [b,e,*]

[a] *Collaborative Innovation Center of Yangtze River Delta Region Green Pharmaceuticals, Zhejiang University of Technology, Hangzhou, Zhejiang, 310014, China*
[b] *The First Affiliated Hospital of Zhejiang Chinese Medical University, Hangzhou, Zhejiang, 310006, China*
[c] *College of Pharmaceutical Science, Zhejiang Chinese Medical University, Hangzhou, Zhejiang, 310053, China*
[d] *Zhejiang Provincial Key Laboratory of TCM for Innovative R&D and Digital Intelligent Manufacturing of TCM Great Health Products, Huzhou, Zhejiang 313200, China*
[e] *Kungen Wang National Famous Chinese Medicine Doctor Studio, Hangzhou, Zhejiang, 310006, China*

ARTICLE INFO

Keywords:
MAFLD
Wang's metabolic formula (WMF)
TCM
Metabolomics
PPAR signaling pathway
Retinol metabolism

ABSTRACT

Wang's metabolic formula (WMF) is a traditional Chinese medicine formula developed under the guidance of Professor Kungen Wang. WMF has been clinically utilized for several years. However, the therapeutic mechanism of WMF in treating metabolic-associated fatty liver disease (MAFLD) remains unclear. In this study, we performed phytochemical analysis on WMF using LC-MS. To study the role of WMF in MAFLD, we orally administered WMF (20.6 g/kg) to male MAFLD mice induced by a high-cholesterol high-fat diet (HCHFD). Then pathological, biochemical, and metabolomic analyses were performed. The main components of WMF are chlorogenic acid,

Abbreviations: ALT, Alanine aminotransferase; AST, Aspartate aminotransferase; BCA, Bicinchoninic acid; BSA, Bovine serum albumin; DAB, 3,3′-diaminobenzidine; DAD, Photodiode-array detection; EA, Epididymis adipose; ELISA, Enzyme linked immunosorbent assay; FLD, Fatty liver disease; GLU, Glucose; H&E, Hematoxylin and eosin; HCHFD, High-cholesterol high-fat diet; HDL-c, High-density lipoprotein cholesterol; HRP, Horseradish peroxidase; IHC, Immunohistochemical; IL, Interleukin; IOD, Integral optical density; KEGG, Kyoto Encyclopedia of Genes and Genomes; LDL-c, Low-density lipoprotein cholesterol; MAFLD, Metabolic-associated fatty liver disease; NAFLD, Non-alcoholic fatty liver disease; NAS, NAFLD/MAFLD activity score; NF, Nuclear factor; OPLS-DA, Orthogonal partial least squares-discriminant analysis; ORO, Oil Red O; PBS, Phosphate buffer saline; PLS-DA, Partial least squares-discriminant analysis; PPAR, Peroxisome proliferators-activated receptor; PPC, Polyene phosphatidylcholine capsules; RAR, Retinoic acid receptor; RIPA, Radio immunoprecipitation assay; RXR, Retinoid X receptor; SDS-PAGE, Sodium dodecyl sulfate polyacrylamide gel electrophoresis; SPF, Specific pathogen free; SREBP-1c, Sterol-regulatory element binding protein-1c; TC, Total cholesterol; TCM, Traditional Chinese Medicine; TG, Triglyceride; TNF, Tumor necrosis factor; VLDLR, Very low-density lipoprotein receptor; WMF, Wang's metabolic formula.

* Corresponding author. The First Affiliated Hospital of Zhejiang Chinese Medical University, Hangzhou, Zhejiang, 310006, China.
** Corresponding author. College of Pharmaceutical Science, Zhejiang Chinese Medical University, Hangzhou, Zhejiang, 310053, China.
*** Corresponding author. The First Affiliated Hospital of Zhejiang Chinese Medical University, Hangzhou, Zhejiang, 310006, China.
**** Corresponding author. The First Affiliated Hospital of Zhejiang Chinese Medical University, Hangzhou, Zhejiang, 310006, China.
E-mail addresses: chensuhong@aliyun.com (S. Chen), 386188129@qq.com (J. Huang), wkg1220@163.com (K. Wang), medcat4@163.com (Y. Zhi), zjtcmlgy@163.com (G. Lv), linda0358@163.com (S. Shen).
[1] These authors contributed equally.

https://doi.org/10.1016/j.heliyon.2024.e33418
Received 15 March 2024; Received in revised form 20 June 2024; Accepted 20 June 2024
Available online 22 June 2024

geniposide, albiflorin, paeoniflorin, and calycosin-7-*O*-glucoside. MAFLD mice treated with WMF exhibited significant improvements in obesity, abnormal lipid metabolism, inflammation, and liver pathology. WMF decreased aspartate aminotransferase (AST), alanine aminotransferase (ALT), and triglyceride (TG) levels in the serum of MAFLD mice while increasing high-density lipoprotein cholesterol (HDL-c) levels. WMF lowered liver TG levels and inflammatory factors (IL-1β, IL-6, TNF-α, and NF-κB). Metabolomic analysis of the liver annotated 78 differentially regulated metabolites enriched in four pathways: glycerophospholipid metabolism, retinol metabolism, PPAR signaling pathway, and choline metabolism. Western blot experiments showed that WMF increased the expression of PPAR-α, PPAR-β, and RXR in the liver while decreasing the expression of RAR. The study demonstrates that WMF has a solid preventive and therapeutic effect on MAFLD. The anti-inflammatory and regulation of abnormal liver metabolism activities of WMF involve retinol metabolism and the PPAR signaling pathway.

1. Introduction

An international panel of experts recently released a consensus statement [1,2], redefining and renaming non-alcoholic fatty liver disease (NAFLD), a term that had been in use for approximately 40 years, as metabolic-associated fatty liver disease (MAFLD). The incidence of MAFLD is continually increasing, especially as obesity, excessive nutrient intake, and nutrient imbalance become more common [3]. The current global prevalence of MAFLD has been estimated at approximately 25 % [4], and the overall prevalence of liver steatosis in adults in China was more than 40 %, making it the country with the highest rates of MAFLD-related diseases, incidence, and annual mortality in Asia [5,6]. If left uncontrolled, it was projected that by 2030, China will have more than 310 million MAFLD patients, making it the country with the highest number of MAFLD patients and liver-related deaths globally [7]. Therefore, in-depth research on the pathogenesis, prevention, and treatment of MAFLD is of significant practical importance.

The etiology and pathogenesis of MAFLD are not yet fully understood. The peroxisome proliferators-activated receptor (PPAR) signaling pathway and retinol metabolism are closely linked to the development of MAFLD. PPARs play crucial roles in various physiological activities, such as energy metabolism, oxidative stress, insulin sensitivity, and inflammation, which are closely associated with the progression of MAFLD [8–11]. Retinol, controlled by retinoid X receptor (RXR) and retinoic acid receptor (RAR), plays a critical role in immunity, embryonic development, and glucolipid metabolism [12–16]. Impairment of retinol metabolism has been observed in the liver of MAFLD [17,18]. Additionally, the expression of RXR, a partner of PPARs and RAR, is reduced in obese individuals, affecting the normal physiological activity of PPARs and RAR [19,20].

Traditional Chinese Medicine (TCM) has been increasingly acknowledged for its promising effects in the management of MAFLD. The potential utility of TCM in this context has been attributed to its advantageous stability, broad scope of therapeutic targets and impacts, and reduced toxicity compared to standard pharmaceutical treatments. Within the framework of TCM, the principle of nourishing the spleen and bolstering the stomach is of critical importance in combating fatty liver disease. Prof. Kungen Wang is a renowned national TCM practitioner and the academic leader in the national field of "Traditional Chinese Medicine for Spleen and Stomach Diseases." Wang's metabolic formula (WMF), including Huangqi (*Astragalus membranaceus*(Fisch.) Bge.), Danshen (*Salvia miltiorrhiza*Bge.), Shanzha (*Crataegus pinnatifida*Bge.), Chishao (*Paeonia lactiflora*Pall.), Xiangfu (*Cyperus rotundus* L.), is derived from Prof. Kun-Gen Wang's clinically effective prescription for the treatment of fatty liver disease (FLD). However, the mechanisms of WMF remain to be thoroughly characterized.

In the domain of TCM pharmacology, metabolomics enables a comprehensive view of the composite effects and principles of compatibility in mixed Chinese herbal remedies [21]. Moreover, metabolomics permits data analysis from multiple scales and perspectives, facilitating the understanding of relationships between the effects of Chinese medicines and the biological factors underlying disease states. This understanding illuminates pharmacodynamic mechanisms, offering fresh insights for deepening studies into disease mechanisms and drug effectiveness.

Thus, the primary purposes of this study were to identify the main components of WMF and to evaluate its therapeutic effects and mechanism. To study the effects of this preparation in vivo, we employed a high-cholesterol, high-fat diet (HCHFD) induced mouse model of MAFLD, and we utilized biochemical, immunological, and histological measurements, in addition to a UPLC-TripleTOF-MS metabolomic profiling approach and Western blot assay. This work lays the foundation for the development of WMF as a new anti-MAFLD product.

2. Materials and methods

2.1. Chemicals and reagents

Polyene phosphatidylcholine capsules (PPC, B/N: BBJD209B) were purchased from Sanofi-Aventis Pharmaceutical Co., Ltd. (Beijing, China). Chlorogenic acid (327-97-9) was purchased from Chengdu Pufei De Biotech Co., Ltd. (Sichuan, China). Geniposide (24512-63-8), paeoniflorin (23180-57-6), albiflorin (39011-90-0), calycosin-7-*O*-glucoside (20633-67-4), and hematoxylin and eosin (H&E) staining solution (R32933) were purchased from Shanghai Yuanye Biotechnology Co., Ltd. (Shanghai, China). Oil Red O (ORO, 1320-06-5) was purchased from BBI CO., Ltd. (Shanghai, China). Test kits for total cholesterol (TC, R202), triglyceride (TG, R201), high-density lipoprotein cholesterol (HDL-c, R203T), glucose (GLU, R108), aspartate aminotransferase (AST, R002), and alanine

aminotransferase (ALT, R001) were purchased from Medicalsystem Biotechnology Co., Ltd. (Zhejiang, China). TC (A111-1-1) and TG (A110-1-1) assay kits were purchased from Nanjing Jiancheng Bioengineering Institute Co., Ltd. (Jiangsu, China). Bicinchoninic acid (BCA) protein concentration determination kit (P0012), Radio immunoprecipitation assay (RIPA) lysis buffer (P0013B), enhanced chemiluminescent assay kit (P0018FS), and 3,3′-diaminobenzidine (DAB, P0202) were obtained from Beyotime Biotechnology Reagent Co., Ltd. (Shanghai, China). Bovine serum albumin (BSA), H_2O_2, horseradish peroxidase (HRP)-conjugated goat anti-rabbit IgG (SV0002), and HRP-conjugated goat anti-mouse IgG (SV0001) were purchased from Boster Biological Technology Co., Ltd. (Zhejiang, China). Enzyme linked immunosorbent assay (ELISA) kits to measure concentrations of interleukin (IL)-1β (MM-0040M1) and tumor necrosis factor (TNF)-α (MM-0132M1) were purchased from Jiangsu Meimian Industrial Co., Ltd. (Jiangsu, China). Antibodies recognizing peroxisome proliferator-activated receptor (PPAR)-α (66826-1-Ig), IL-6 (66146-1-Ig), and nuclear factor (NF)-κB (66535-1-Ig) and HRP-conjugated affinipure goat anti-rabbit IgG (H + L) (SA00001-2) and HRP-conjugated affinipure goat anti-mouse IgG (H + L) (SA00001-1) antibodies were purchased from Proteintech Group Inc. (Illinois, USA). PPAR-β (sc-74517), RAR (sc-514585), and RXR (sc-46659) antibodies were purchased from Santa Cruz Biotechnology Co., Ltd. (Shanghai, China). No-stain protein labeling reagent (A44717) was purchased from Thermo Fisher Scientific Inc. (Massachusetts, USA).

All herbs in the WMF prescription, including Huangqi, Danshen, Shanzha, Chishao, and Xiangfu, were purchased from Zhejiang Tiandao Pharmaceutical Co., Ltd. (Zhejiang, China). The voucher specimen (WMF202110) was stored in the Research and Development Laboratory of Traditional Chinese Medicine Health Products, Zhejiang University of Technology.

2.2. Animals

Forty SPF male ICR mice (6–8 weeks old, 25 ± 2 g) were purchased from the Zhejiang Academy of Medical Science (SCXK(Zhe) 2019-0002) and raised in the Animal Center of Zhejiang University of Technology. All animal experimental procedures were conducted in accordance with the Guide for the Care and Use of Laboratory Animals in the Zhejiang University of Technology and conformed to the National Institutes of Health Guide for Care and Use of Laboratory Animals (Publication No. 85-23, revised 1996).

2.3. Identification of the main constituents of WMF

2.3.1. Preparation of WMF

WMF was prepared by the Institute of TCM and Health Products of Zhejiang University of Technology. The herbs were soaked in pure water and then heated to reflux for 1 h. The sample was filtered, and the residue was boiled in pure water and filtered again. The two filtrates were combined and concentrated by a rotary vacuum evaporator at a temperature of 50 °C to a concentration of 2.06 g/mL to obtain the crude herb, which was refrigerated for later use.

2.3.2. LC-MS analysis

WMF was analyzed using Agilent 1260 series HPLC with photodiode-array detection (DAD; Agilent, USA) equipped with an Eclipse XDB-C18 column (4.6 mm × 250 mm, 5 μm; Agilent, USA), and Agilent 6546 Q-TOF system.

The LC conditions were set as follows: the column temperature was set at 30 °C. The detection wavelength was set at 244 nm. The mobile phase consisted of acetonitrile (A) and 0.1 % phosphoric acid aqueous solution (B). The gradient elution procedure was as follows: 0–5 min, 5 % A; 5–10 min, 5–10 % A; 10–45 min, 10–22 % A; 45–50 min, 22–28 % A; 50–60 min, 28–30 % A; 60–70 min, 30 %–100 % A; and 70–80 min, 100 to 5 % A. The flow rate was 1 mL/min, and the injection volume was 10 μL.

The MS conditions were set as follows: the mass spectrometer was operated in negative ion scanning mode; the gas temperature was 300 °C; the drying gas flow rate was 8 L/min; the nebulizer was 30 psi; the sheath gas temperature was 300 °C; the sheath gas flow rate was 11 L/min; the capillary, nozzle, fragmentor, skimmer, and OCT 1 RF Vpp voltages were 4000 V, 1000 V, 175 V, 65 V, and 750 V, respectively; and the MS scanning range was 50–1500 *m/z*.

2.3.3. Identification of the main constituents

A database of WMF constituents was constructed by searching the published papers [22–25] and HERB (http://herb.ac.cn/), ETCM (http://www.tcmip.cn/ETCM/), and PubChem (https://pubchem.ncbi.nlm.nih.gov/) databases. The candidate substances were then narrowed down by molecular formulas generated from spectrum peak with Qualitative Navigator (Agilent, USA). The annotated constituents were identified and quantified with reference standards.

2.4. Animals modeling of MAFLD and treatment

Our group previously established that the ideal concentration of WMF for treating dyslipidemia rats is 14.28 g/kg (Supplementary Table 1, Supplementary Fig. 1A-F). This was converted to a dosage of 136.0 g/d for a 60-kg adult. Additionally, for this study, the dosage for mice was determined to be 20.6 g/kg.

Considering the experimental animals' lifespan and the optimal dosage determined, we used a single dosage in this study. After one week of acclimation, a total of 40 ICR mice were randomly divided into 4 groups (n = 10): a normal control group (NC), a model control group (MC), a PPC group (PPC, 205.4 mg/kg, i.g., qd.), and a WMF extract group (WMF, 20.6 g/kg (crude herb), i.g., qd.). All groups except the NC group were fed an HCHFD for 17 weeks, and drugs were administered while modeling. HCHFD chow, which contained 10 % lard, 10 % egg yolk powder, 5 % sugar, 2 % cholesterol, and 0.5 % cholate, was obtained from Trophic Animal Feed High-Tech Co., Ltd. (Jiangsu, China).

During the experimental period, the mice were weighed once per week. At the end of the experiment, the mice were fasted overnight, and blood was obtained from the ophthalmic venous plexus. The blood was centrifuged at 3000 rpm for 10 min twice to obtain serum for biochemical analysis. After blood sampling, the mice were sacrificed under anesthesia, and the liver and epididymis adipose (EA) tissue were rapidly removed and weighed. EA and part of the liver were fixed in a 10 % formalin solution. Another part of the liver was immersed in a 30 % sucrose solution for pathological analyses. The remaining parts of the liver were stored at −80 °C for determination of hepatic lipids, metabolomics, and Western blot analyses.

Tissue/Organ index (%) = Tissue/Organ weight (g) ÷ Body weight (g)

2.5. Serum biochemical assays

The levels of TC, TG, HDL-c, GLU, AST, and ALT in serum were determined with a Hitachi 7020 Automatic Analyzer. Low-density lipoprotein cholesterol (LDL-c) levels were calculated using the Friedewald formula [26].

2.6. Measurement of lipids in liver

Liver tissues (~100 mg), were placed into ice-cold ethanol and then homogenized to prepare a 10 % (w/v) homogenate. This sample was centrifuged at 2500 rpm for 10 min, and the levels of TC and TG in the supernatant were determined using assay kits, according to the manufacturer's instructions.

2.7. ELISA analysis

Liver tissues (~80 mg), were homogenized in ice-cold phosphate buffer saline (PBS, 0.01 M, pH = 7.4) to prepare a 10 % (w/v) homogenate, which was centrifuged at 5000 g for 5 min. ELISA kits were used to determine the levels of IL-1β and TNF-α in the supernatant, according to the manufacturer's instructions.

2.8. Histological staining of liver section

Oil Red O staining to identify lipid accumulation and H&E staining were performed as described in our previous reports [27,28]. Briefly, liver tissue was fixed with 30 % sucrose solution before embedding into optimal cutting temperature compound (Sakura, Japan). The tissue was then cut into 10 μm frozen sections. The cryosections were stained with 0.5 % Oil Red O solution, and the nuclei were counterstained with hematoxylin. The stained sections were photographed with an Olympus BX43 light microscope (Olympus, Japan) and analyzed with Image-Pro Plus. The hepatic pathology was scored as described in Table 1 [29].

2.9. Immunohistochemical (IHC) analysis of inflammatory cytokines in liver

The expression and localization of NF-κB p65 and IL-6 in the liver were determined by immunohistochemical staining according to a previous report [30]. The tissue sections were incubated with anti–NF–κB p65 or anti-IL-6 antibodies (diluted 1:200 in PBS (0.01 M)) at 4 °C overnight. Then, the sections were incubated in HRP-conjugated affinipure goat anti-mouse/rabbit IgG (H + L) antibodies and developed color with DAB. The sections were observed under a light microscope, and the levels of protein expression in positively stained regions of the section were analyzed using semi-quantitative integrated optical density analysis with Image J.

2.10. Liver metabolomics analysis

2.10.1. Metabolite extraction

Each liver sample (approximately 500 mg wet weight) was added to a 2 mL centrifuge tube, and a 6 mm diameter grinding bead was added. A 400 μL aliquot of extraction solution (methanol:water, 4:1 (v:v)) containing 0.02 mg/mL of internal standard (L-2-chlorophenylalanine) was added, and the sample was ground with a Wonbio-96c frozen tissue grinder (Shanghai Wanbo Biotechnology Co., Ltd., China) for 6 min (−10 °C, 50 Hz). The sample was further processed three times with low-temperature ultrasonic extractions (0 °C, 40 kHz, 15 min). The samples were incubated at −20 °C for 20 min and then centrifuged for 10 min at 4 °C and 13,000 rpm. The supernatant was transferred to an injection vial for LC-MS/MS analysis.

Table 1
Scoring standard of NAFLD/MAFLD activity.

NAS (0–8 points)					
1.Steatosis (0-3 points)		2. Lobular inflammation (0-3 points)		3. Ballooning (0-2 points)	
0	<5 %	0	No foci	0	None
1	5-33 %	1	<2 foci per 200 × field	1	Few balloon cells
2	33-66 %	2	2-4 foci per 200 × field	2	Many cells/prominent ballooning
3	>66 %	3	>4 foci per 200 × field		

2.10.2. LC-MS analysis

LC-MS analyses were performed using an UPLC-TripleTOF 5600 system (AB Sciex, USA) equipped with a UPLC BEH C18 column (100 × 2.1 mm, 1.7 μm; Waters, USA) and an electrospray ionization source operating in positive mode (ESI^+) and negative mode (ESI^-). The column temperature was set at 40 °C, the sample injection volume was 20 μL, and the flow rate was 0.40 mL/min. The mobile phase consisted of 0.1 % (v/v) formic acid (A) and acetonitrile-isopropanol (1:1, containing 0.1 % (v/v) formic acid). The gradient elution procedure was as follows: 0–3 min, 100 to 80 % A; 3–9 min, 80 to 40 % A; 9–11 min, 40 to 0 % A; 11–13.5 min, 0 % A; 13.5–13.6 min, 0–100 % A; and 13.6–16 min, 100 % A.

The MS conditions were set as follows: the mass spectrometer was operated in positive and negative ion scanning modes; the electrospray capillary voltage was 1.0 kV; the injection voltage was 40 V; the collision voltage was 6 eV; the ion source temperature was 120 °C; the desolvation temperature was 500 °C; the carrier gas flow rate was 900 L/h; the MS scanning range was 50–1000 *m/z*; and the resolution was 30,000.

2.10.3. Data analysis

LC/MS raw data was pretreated with Progenesis QI (Waters, USA). Metabolites were annotated by searching the databases HMDB (http://www.hmdb.ca/), Metlin (https://metlin.scripps.edu/), and Majorbio Database. The partial least squares-discriminant analysis (PLS-DA) and orthogonal PLS-DA (OPLS-DA) were performed using MetaboAnalyst (https://www.metaboanalyst.ca/) and Majorbio Cloud (http://cloud.majorbio.com) [31].

2.11. Western blot assay

Liver tissue samples (~80 mg) were lysed at 4 °C in RIPA lysis buffer. The tissue homogenates were centrifuged at 12,000 rpm for 10 min at 4 °C. Concentrations of total proteins in the supernatants were determined with the BCA assay. Proteins were separated with

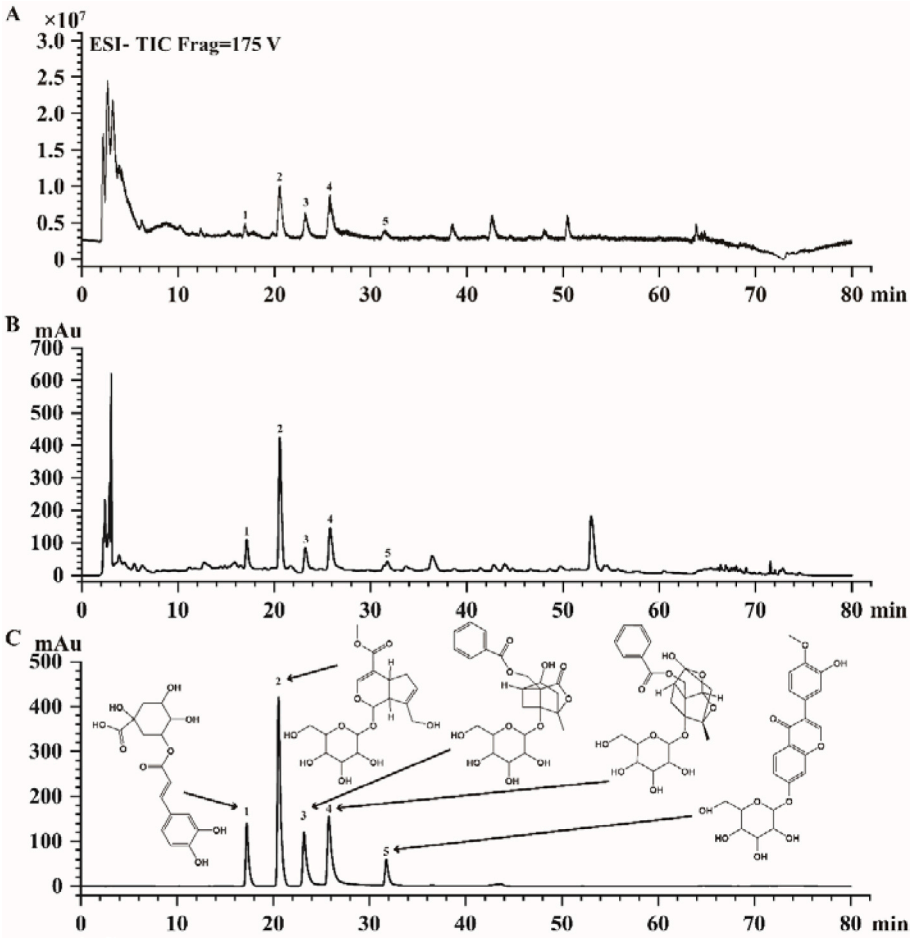

Fig. 1. LC-MS analysis of WMF. (A) Total ion chromatograms(TIC) of WMF in ESI^- mode. (B) Representative liquid chromatogram of WMF extract. (C) Representative liquid chromatogram of mixed standards. 1 = chlorogenic acid, 2 = geniposide, 3 = alibiflorin, 4 = paeoniflorin, 5 = calycosin 7-*O*-glucoside with retention time 17.227 min, 20.537 min, 23.191 min, 25.760 min, 31.731 min, respectively.

10 % SDS-PAGE and transferred onto polyvinylidene fluoride membranes. The membranes were washed in pure water and then incubated with No-Stain protein labeling reagent for 10 min. The total protein was visualized with an Invitrogen iBright FL1500 imaging system (Thermo Fisher, USA).

The membranes were then blocked with 5 % non-fat milk for 2 h at room temperature and incubated with primary antibodies (anti-PPAR-α 1:1000, anti-PPAR-β 1:500, anti-RXR 1:500, or anti-RAR 1:500) overnight at 4 °C. After being washed in TBST, the membranes were incubated with HRP-conjugated goat anti-rabbit or mouse secondary antibodies (1:10000) for 1 h at room temperature and washed again. The protein bands were detected using an enhanced chemiluminescent assay kit. Protein expression levels were quantified by densitometry and normalized to total protein with ImageJ.

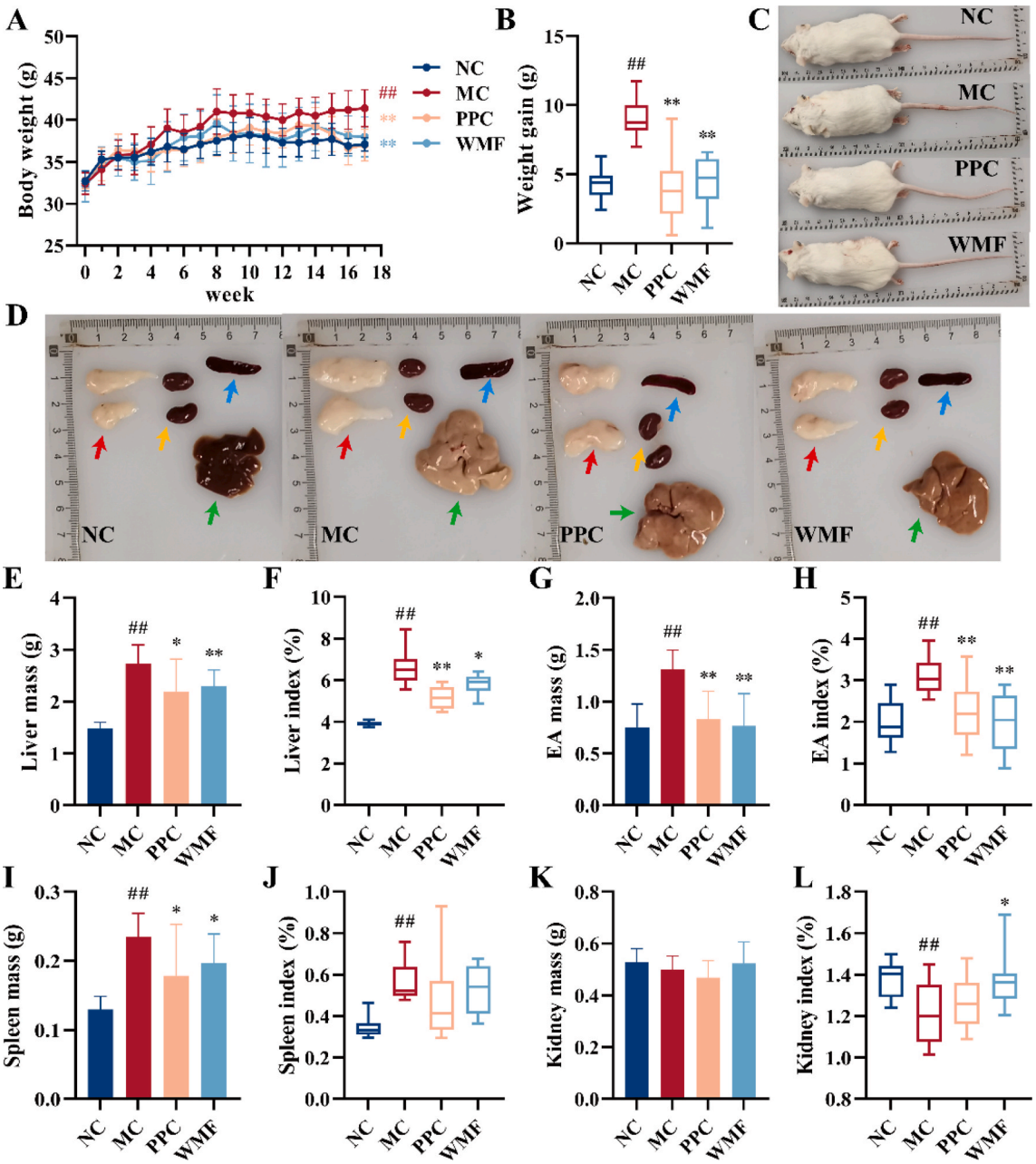

Fig. 2. WMF slowed the weight and alleviated fat accumulation in MAFLD mice. (A) Body weight change. (B) Weight gain in 17 weeks. (C) Representative photograph of mice appearance. (D) Representative photograph of major organs and tissues. (E–F) Liver mass and index. (G–H) EA mass and index. (I–J) Spleen mass and index. (K–L) Kidney mass and index. Red arrow = EA; yellow arrow = kidney; blue arrow = spleen. green arrow = liver. All the values were presented as the mean ± SD. $^{\#\#}P < 0.01$ vs. NC group; $^{*}P < 0.05$, $^{**}P < 0.01$ vs. MC group. (n = 10).

2.12. Statistical analysis

All data were expressed as mean ± standard deviation (SD). SPSS 19.0 and GraphPad Prism 9.5.0 were used to analyze and visualize the data. Statistical analysis was performed using one-way analysis of variance (ANOVA). Independent-sample *t*-test was used to compare difference between two groups. $P < 0.05$ was considered to be statistically significant.

3. Results

3.1. LC-MS analysis of WMF components

LC-MS analysis of the WMF extract was performed to narrow down the candidate substances (Fig. 1A). HPLC-DAD analysis compared the retention times of major peaks arising from the sample with those of authentic reference compounds (Fig. 1B–C). As shown in Fig. 1, these analyses led to the identification of five major compounds: chlorogenic acid, geniposide, albiflorin, paeoniflorin, and calycosin-7-*O*-glucoside. The levels of chlorogenic acid, geniposide, albiflorin, paeoniflorin, and calycosin-7-*O*-glucoside in the extract were 4.06 mg/g, 6.16 mg/g, 3.97 mg/g, 5.25 mg/g, and 0.14 mg/g, respectively.

3.2. WMF mitigates the pathological signs of MAFLD mice

A mouse model of MAFLD was developed by feeding mice with an HCHFD for 17 weeks. The average weights of the body, liver, EA, and spleen of model mice were significantly higher than those of the normal control group ($P < 0.01$; Fig. 2C-D). PPC is known to be an effective treatment for MAFLD, and treatment of mice fed the same HCHFD with PPC led to significantly decreased body weight after 17 weeks ($P < 0.01$; Fig. 2A–B). Similarly, treatment with WMF extract led to significantly decreased body weight after 17 weeks on the HCHFD ($P < 0.01$; Fig. 2A–B). Treatment with WMF also was associated with significantly reduced liver mass ($P < 0.01$), liver index ($P < 0.05$), EA mass ($P < 0.01$), EA index ($P < 0.01$), spleen mass ($P < 0.05$), and significantly increased kidney index ($P < 0.05$) as compared to untreated model mice (Fig. 2E–L). These results indicated that treatment of mice with WMF is associated with reductions of the abnormal weight gain and the abnormal visceral fat accumulation associated with HCHFD-induced MAFLD.

3.3. WMF attenuates MAFLD-associated changes to serum lipid, glucose, and transaminase levels

Mice in the model group exhibited significantly higher serum TC, TG, LDL-c, and GLU levels as compared to normal control mice ($P < 0.01$, 0.05; Fig. 3A-B, D-E), and the serum ALT and AST activities were also significantly higher in model mice ($P < 0.01$; Fig. 3F–G). Conversely, the serum HDL-c level in model mice was significantly lower than that in normal control mice ($P < 0.01$; Fig. 3C). WMF

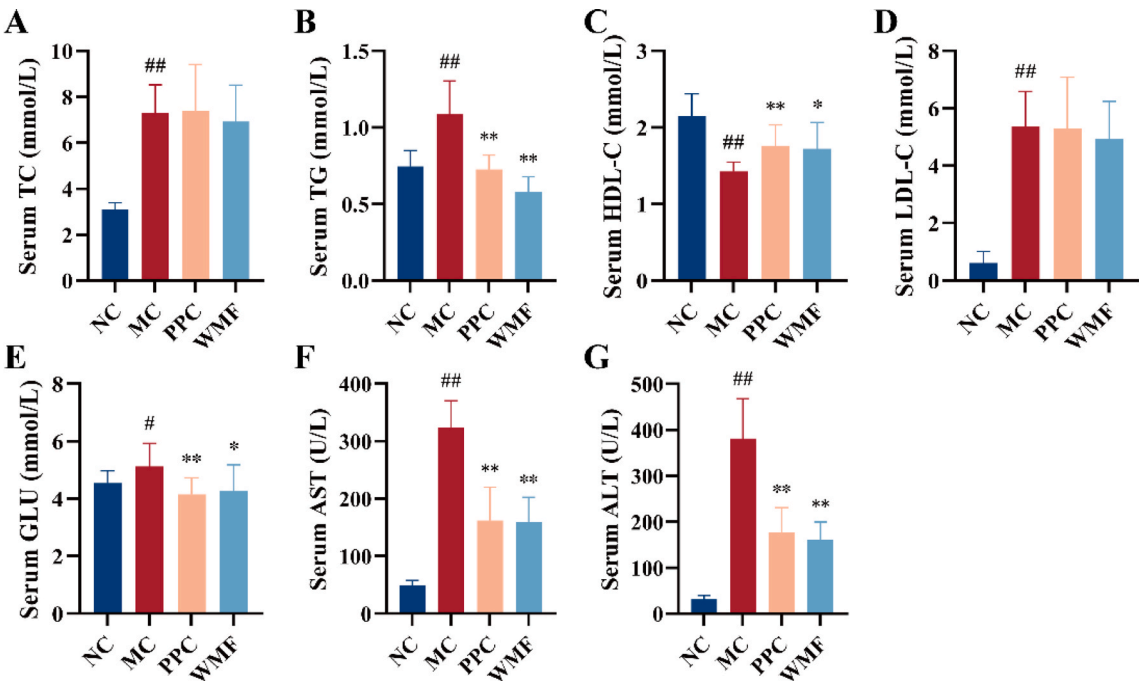

Fig. 3. Effect of WMF on serum biochemistry. (A–G) The levels of TC, TG, HDL-C, LDL-C, GLU, AST, and ALT in the serum, respectively. All the values were presented as the mean ± SD. $^{\#}P < 0.05$, $^{\#\#}P < 0.01$ vs. NC group; $^{*}P < 0.05$, $^{**}P < 0.01$ vs. MC group. (n = 10).

treatment significantly suppressed the HCHFD-induced increases in serum TG, AST, ALT, and GLU levels ($P < 0.01$, 0.05) as well as the decrease in serum HDL-c ($P < 0.05$). The results showed that treatment with WMF is associated with beneficial effects on the levels of TG, HDL-c, and GLU in mouse models, improved abnormalities of glucose and lipid metabolism and reduced serum AST and ALT levels. These suggest that WMF might have the potential to improve liver function.

3.4. WMF alleviates MAFLD-associated changes to hepatic lipid levels

The HCHFD induced hepatic steatosis and inflammatory cell infiltration as evidenced by imaging of H&E− and Oil Red O-stained sections of liver tissues (Fig. 4A). Treatment with WMF or PPC improved hepatic steatosis and diminished the infiltration of inflammatory cells, and they were both associated with significantly reduced the NAFLD/MAFLD activity score (NAS; $P < 0.01$; Fig. 4A–C).

On a molecular level, the concentrations of TC and TG within the liver were significantly increased in model mice relative to normal control mice ($P < 0.01$). The liver TC content was significantly decreased by treatment with PPC ($P < 0.05$), treatment of model mice with WMF was not associated with a significant change in liver TC content (Fig. 4D). Conversely, the liver TG content of model mice was significantly attenuated by treatment with WMF ($P < 0.01$), but not by PPC (Fig. 4E). Collectively, these results suggest that WMF treatment attenuates HCHFD-induced liver steatosis in mice.

3.5. WMF ameliorates MAFLD-associated liver inflammation

IHC was used to investigate the impacts of MAFLD and the treatments on inflammation by quantifying the expression of the inflammatory markers IL-6, IL-1β, NF-κB, and TNF-α in liver tissues. Compared with normal control mice, the livers of model mice exhibited significantly higher levels of expression of IL-6, NF-κB, IL-1β ($P < 0.01$; Fig. 5A-D), and TNF-α ($P < 0.05$; Fig. 5E). Treatment of model mice with WMF was associated with significant reductions in the levels of IL-6, NF-κB, IL-1β, and TNF-α ($P < 0.01$). Treatment with PPC was associated with significant reductions of IL-6, NF-κB, and IL-1β ($P < 0.01$). These results suggested that WMF exerts an anti-inflammatory effect in the livers of MAFLD mice by reducing hepatic inflammatory cytokines.

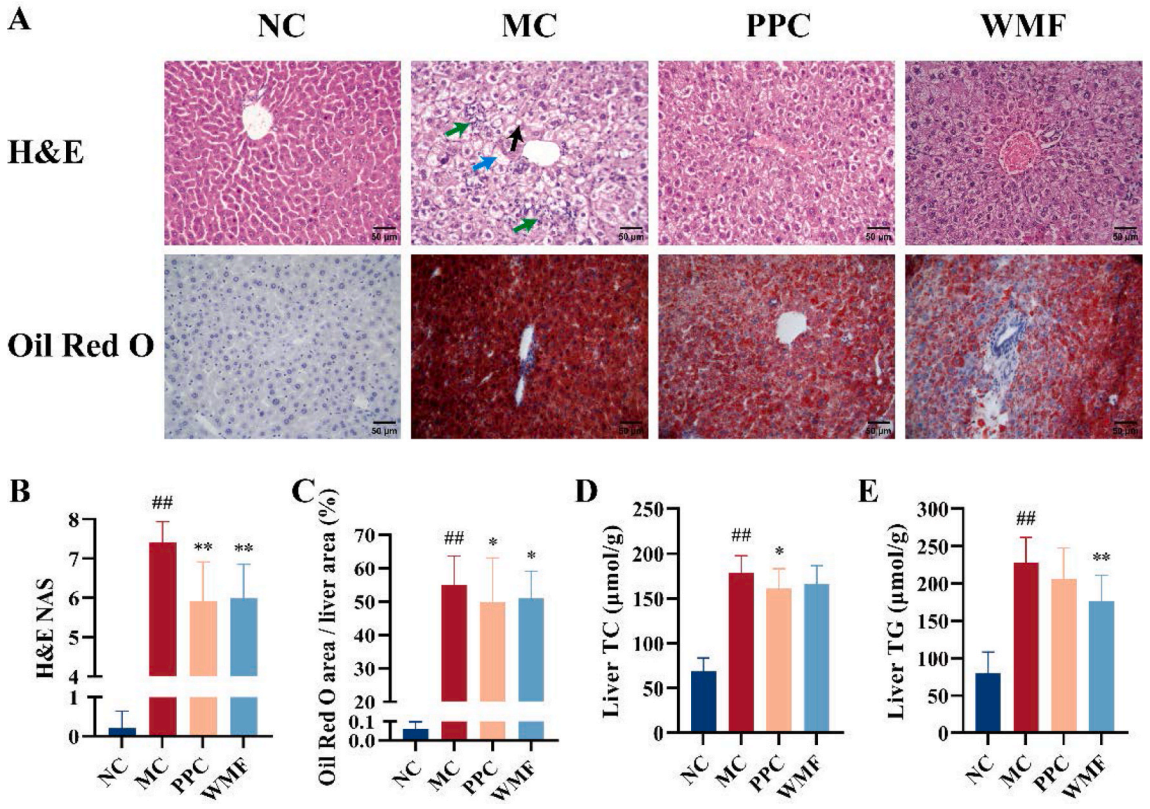

Fig. 4. Effect of WMF on liver steatosis. (A) Representative photomicrograph of histopathological changes in the liver (H&E 400 × ; Oil Red O 400 ×). (B) NAFLD/MAFLD activity score. (C) Percentage of Oil Red O staining area. (D) The TC levels in the livers. (E) The TG levels in the livers. Bar = 50 μm; black arrow = lipid droplet; green arrow = inflammatory cell infiltration; blue arrow = ballooning degeneration. All the values were presented as the mean ± SD. $^{\#\#}P < 0.01$ vs. NC group; $^{*}P < 0.05$, $^{**}P < 0.01$ vs. MC group. (n = 10). (For interpretation of the references to color in this figure legend, the reader is referred to the Web version of this article.)

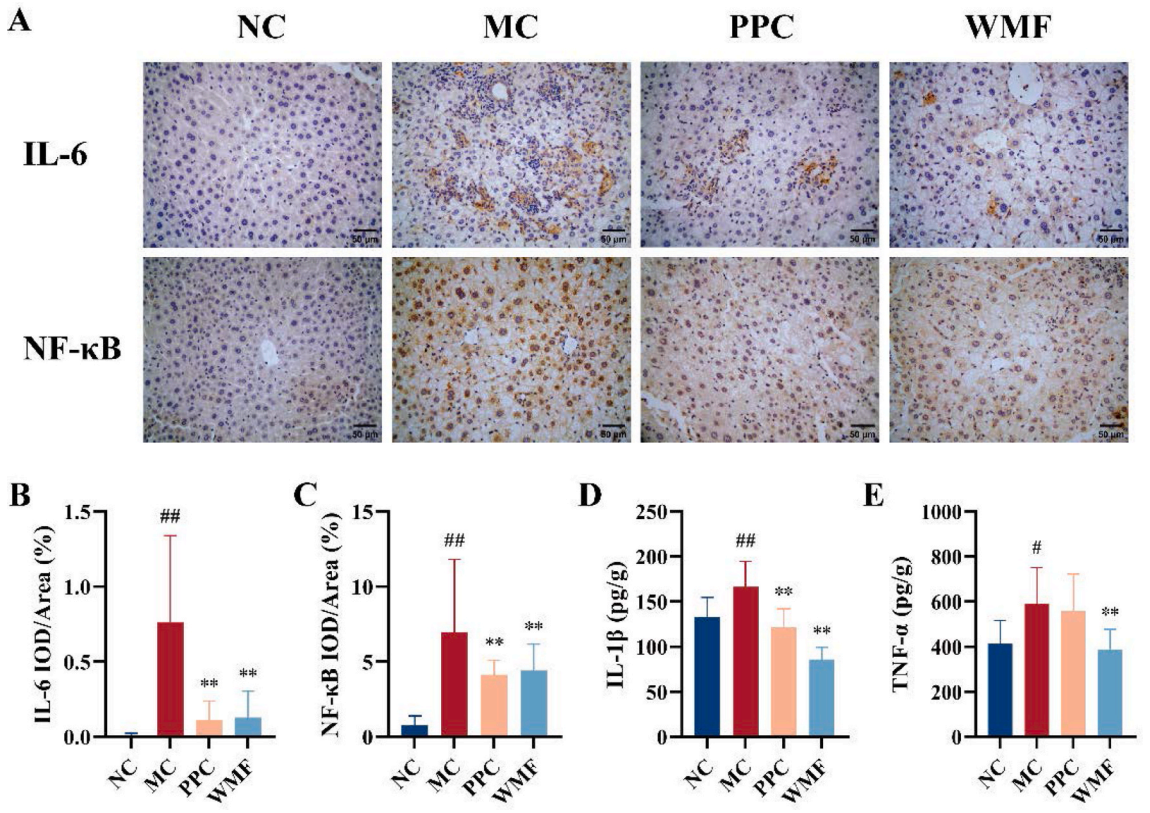

Fig. 5. Effect of WMF on liver inflammation. (A) Representative photomicrograph of liver IL-6 and NF-κB protein expression by IHC. (B) Relative optical density of liver IL-6. (C) Relative optical density of liver NF-κB. (D) The IL-1β levels in the liver. (E) The TNF-α levels in the liver. Bar = 50 μm. All the values were presented as the mean ± SD. $^{\#}P < 0.05$, $^{\#\#}P < 0.01$ vs. NC group; $^{**}P < 0.01$ vs. MC group. (n = 10).

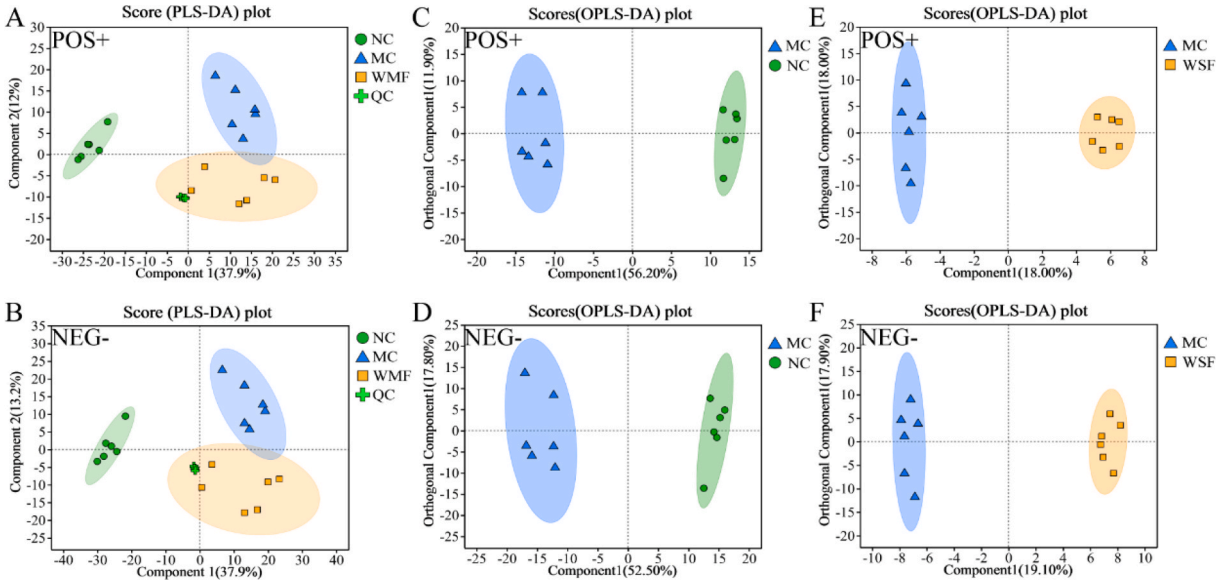

Fig. 6. Untargeted metabolomics analysis of liver. (A–B) PLS-DA score plot in ESI^+ and ESI^- mode. (C) OPLS-DA score plot in ESI^+ and ESI^- mode between NC group and MC group. (E) OPLS-DA score plot in ESI^+ and ESI^- mode between MC group and WMF group. (n = 6).

3.6. WMF restores altered liver metabolite profiles

3.6.1. Assessing metabolic differentiation

The effects of WMF on the liver in the MAFLD model were further explored by analyzing metabolites in the livers of mice using LC-MS. PLS-DA was first performed on metabolites annotated in ESI^+ and ESI^- (Fig. 6A-B). QC samples were clustered in the central area, confirming the stability of the experimental system. The cross-validation and permutation tests indicated that the models had good predictive ability and reliability (Supplementary Fig. 2A-D).

When metabolites from extracts of livers from normal control mice, model mice, and model mice treated with WMF were plotted as differently colored dots (Fig. 6A–B), metabolites from the three groups were clearly divided into three different areas, indicating that the metabolites in the three groups were different. Notably, the group of dots representing metabolites from model mice treated with WMF were located between those of the normal control and model mice, suggesting that treatment with WMF might alter the metabolites present in model mice towards normal levels.

We performed OPLS-DA on data obtained in ESI^+ and ESI^- modes to differentiate the metabolite features further and to screen for potential marker metabolites. The model overview and permutation tests indicated that the models were valid (Supplementary Fig. 2E-L). In the score plots of the OPLS-DA models, metabolites from model mice were separated from those of normal control mice and those of model mice treated with WMF (Fig. 6C–F). These differences suggested that metabolic perturbation had occurred in model mice and that WMF could partially alleviate this metabolic perturbation.

3.6.2. Therapeutic mechanism screening and pathway enrichment

OPLS-DA S-plots were constructed to investigate differential metabolite profiles that can be used to distinguish model mice treated with WMF from normal control mice and from untreated model mice; such distinguishing metabolites may be regarded as potential therapeutic mechanisms associated with successful WMF treatment (Fig. 7A-B). As defined by VIP >1, $P < 0.05$, and $|FC| > 1$, there were 417 differential metabolites annotated between the model and normal control groups and 257 differential metabolites between the WMF-treated model group and the untreated model group. Of 96 common metabolites in these two groups of differential metabolites, the levels of 78 metabolites were altered toward the normal levels by WMF. These 78 metabolites thus were regarded as potential therapeutic mechanisms of WMF against MAFLD (Fig. 7C). Among these 78 metabolites, WMF up-regulated 56 metabolites and down-regulated 22 metabolites (Fig. 7D–Supplementary Table 2).

Kyoto Encyclopedia of Genes and Genomes (KEGG) enrichment and KEGG topology analyses were performed on the 78 annotated metabolites using the criteria $P < 0.05$ and rich factor >0.1 or impact value > 0.1. These analyses demonstrated that the metabolites are involved in four major metabolic pathways: glycerophospholipid metabolism, retinol metabolism, the PPAR signaling pathway, and choline metabolism(Fig. 8A-B). Specifically, WMF significantly reduced the abundance of glycerol 3-phosphate and LysoPC(P-18:1(9Z)/0:0) in the livers of MAFLD model mice ($P < 0.05$, 0.01; Fig. 8C, F); both of these lipids are involved in glycerophospholipid metabolism and choline metabolism. WMF treatment significantly improved retinol metabolism, as the abundance of retinol in the

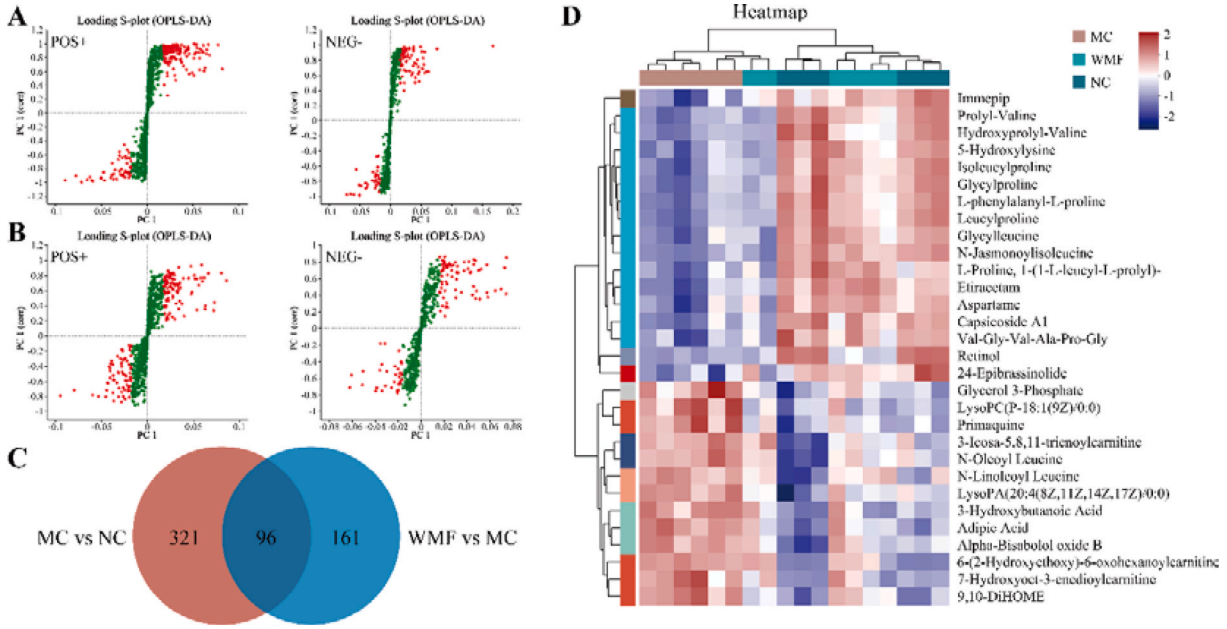

Fig. 7. Differential metabolites among groups. (A) S-plot of metabolites in ESI^+ and ESI^- modes between NC group and MC group. (B) S-plot of metabolites in ESI^+ and ESI^- modes between MC group and WMF group. (C) Common differential metabolites among NC, MC, and WMF groups. (D) Heatmap tree of TOP 30 common differential metabolites. (n = 6).

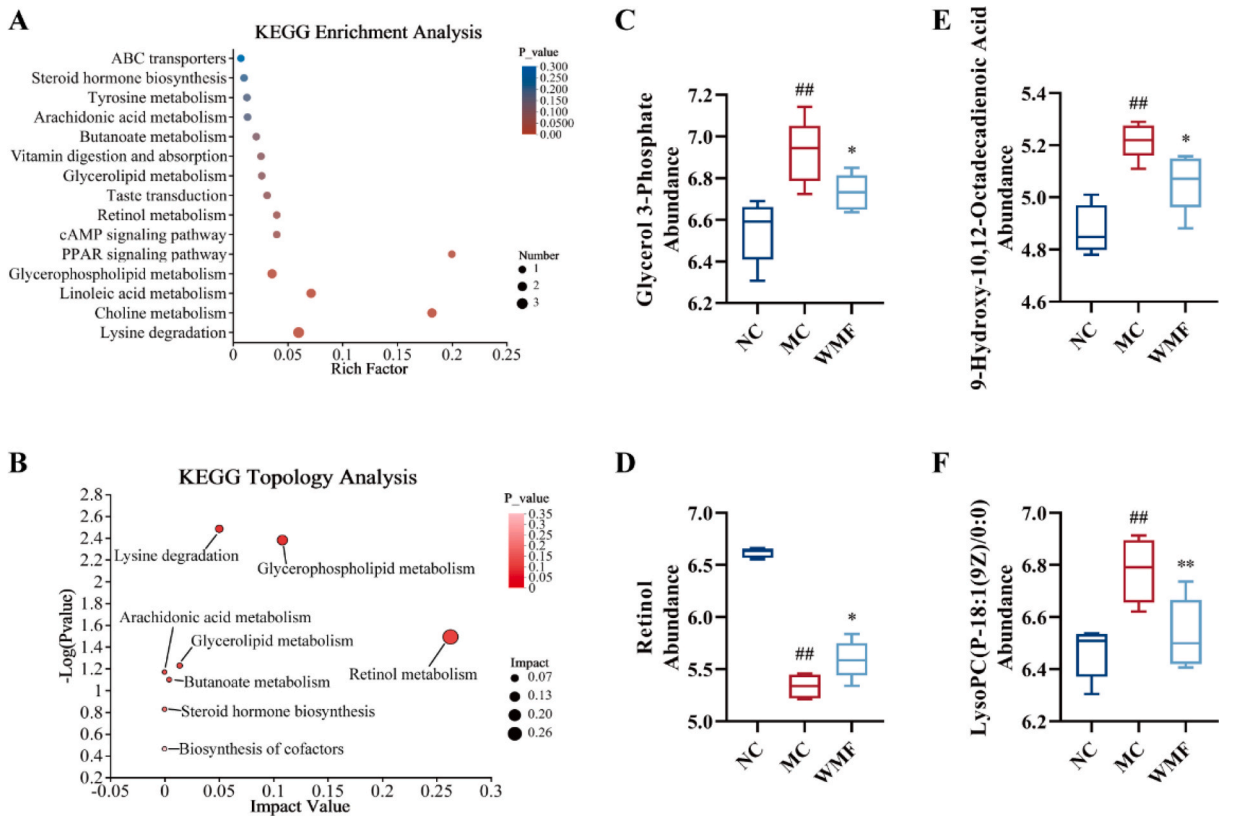

Fig. 8. Summary of pathways analysis in the liver. (A) KEGG enrichment analysis. (B) KEGG topology analysis (C) Abundance of Glycerol 3-Phosphate. (D) Abundance of retinol. (E) Abundance of 9-Hydroxy-10,12-Octadecadienoic Acid. (F) Abundance of LysoPC(P-18:1(9Z)/0:0). All the values were presented as the mean ± SD. $^{\#\#}P < 0.01$ vs. NC group; $^{*}P < 0.05$, $^{**}P < 0.01$ vs. MC group. (n = 6).

liver significantly increased ($P < 0.05$; Fig. 8D). Treatment with WMF was also associated with a reduction of the abundance of 9-hydroxy-10,12-octadecadienoic acid ($P < 0.05$; Fig. 8E), which is associated with the PPAR signaling pathway.

According to this metabolomics study, MAFLD is associated with a disturbance of several key metabolites and metabolic pathways. Importantly, treatment with WMF can partially offset this disturbance, suggesting another potential mechanism leading to WMF's effectiveness in treating MAFLD.

3.7. Effects of WMF on the expression of proteins associated with PPAR signaling

Because our metabolomics analysis suggested that the effect of WMF on MAFLD may occur at least partly through regulation of PPAR signaling, we used Western blotting to investigate the impacts of HCHFD and WMF treatment on the levels of several PPAR-associated proteins in the mouse liver. Key Western blotting results are displayed in Fig. 9A, and the full blots are presented in Supplementary Fig. 3-6. This analysis demonstrated that HCHFD induced significant decreases in the expression of RXR, PPAR-α, and PPAR-β ($P < 0.01$; Fig. 9B-D) and a significant increase in the expression of RAR ($P < 0.01$; Fig. 9E). However, as compared to the levels in the untreated model mice, WMF treatment was associated with significant increases in the levels of RXR, PPAR-α, and PPAR-β ($P < 0.05$; Fig. 9B–D) and a significant decrease in the level of RAR ($P < 0.01$; Fig. 9E) in the liver. Thus, treatment with WMF partially restored the changes in the expression of these proteins observed in MAFLD model mice.

4. Discussion

MAFLD, a type of chronic liver disease, is characterized by hepatic steatosis in combination with obesity, type 2 diabetes, or at least two metabolic risk abnormalities [1]. In healthy populations, the annual incidence rate of MAFLD is approximately 4 %. Currently, the global prevalence of MAFLD is around 25 %, and in the overweight/obese population, it can reach up to 39 % [32,33]. Importantly, besides liver cancer, MAFLD also increases the risk of extrahepatic malignant tumors, showing a significant correlation with colon cancer, adenocarcinoma, thyroid cancer, lung cancer, prostate cancer, and urologic cancers [34].

Among the constituent herbs of WMF, Huangqi, Chishao, Xiangfu, and Shanzha have a long history of application, and are listed in the "Catalog of Substances That Are Both Food and Chinese Herbal Medicine According to Tradition" issued by the State Council of China, [35,36] which indicates the safety of these herbs. Adverse reaction reports for Danshen have focused on its injectable

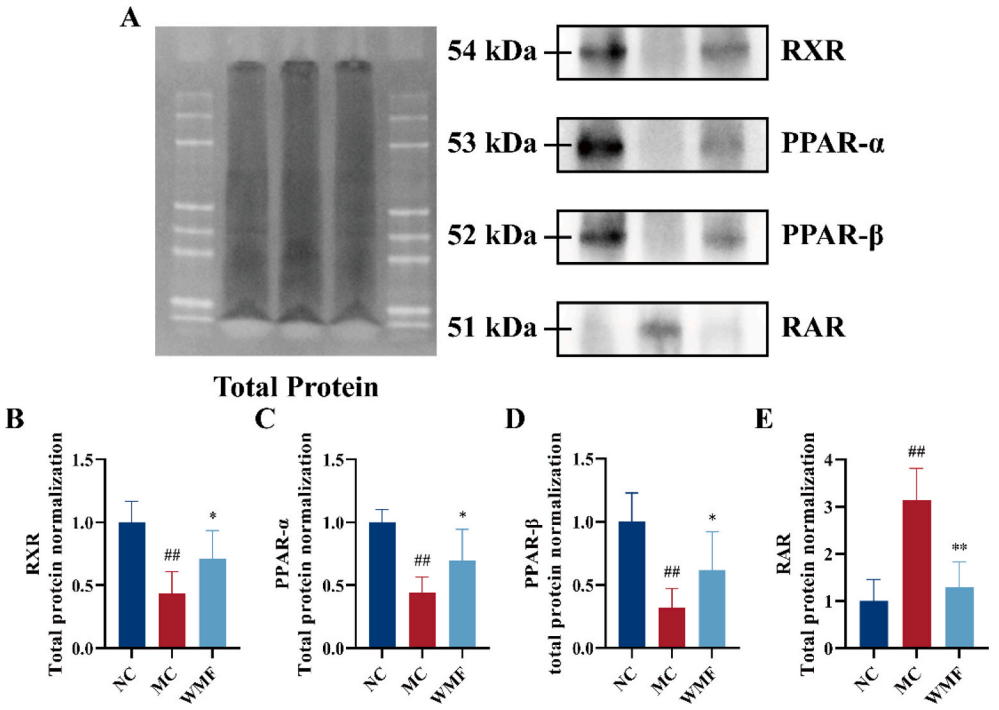

Fig. 9. The effect of WMF on the PPAR signaling pathway and retinol metabolism. (A) Western blot analysis of key proteins of the PPAR signaling pathway and retinol metabolism in various groups. (B–E) Protein blotting analysis of the expression of RXR, PPAR-α, PPAR-β, and RAR, respectively. All the values were presented as the mean ± SD. $^{\#\#}P < 0.01$ vs. NC group; $^{*}P < 0.05$, $^{**}P < 0.01$ vs. MC group. (n = 5).

formulations. The most common adverse reactions were rash and dermatitis [37,38]. In the present study, WMF was found to improve liver weight and spleen weight in MAFLD, with no significant effect on the kidney.

Consistent with our previously published findings [39], our present investigation demonstrated that mice subjected to HCHFD induction for 17 weeks developed dyslipidemia, increased serum transaminase activity, hepatic lipid accumulation, and inflammation. Further examination of the impact of WMF in MAFLD mice revealed additional important findings. The model mice showed decreased body weight, improved metabolic disorders, and reduced inflammation in the liver after treatment with WMF. These results demonstrate the efficacy of WMF in mitigating MAFLD. There is still much work we can accomplish to elucidate the efficacy of WMF further. We are curious about the efficacy of WMF on type 2 diabetes, hypertension, hyperuricemia, atherosclerosis, liver fibrosis, and hepatocellular carcinoma. The efficacy of WMF will be further investigated in the future using a variety of animals and models to explore the range of indications.

A metabolomic study of the liver was conducted to study WMF's mechanism of action further. The results showed that WMF altered 78 metabolites toward normal levels. KEGG analysis demonstrated four pathways that may influence MAFLD: glycerophospholipid metabolism, retinol metabolism, the PPAR signaling pathway, and choline metabolism. In subsequent experiments, we focused on the PPAR signaling pathway and retinol metabolism as the validation targets. WMF increased the expression of PPAR-α, PPAR-β, and RXR in the liver, while decreasing the expression of RAR.

PPAR plays a key role in lipid and glucose metabolism by regulating energy homeostasis, inflammation and fibrosis [40]. Reduced PPAR-α expression in the liver is associated with the development of MAFLD [9]. Activation of PPAR-α accelerates fatty acid β-oxidation, reduces nonestesterified fatty acid, and decreases sterol-regulatory element binding protein-1c (SREBP-1c) expression [41–43]. It has been shown that PPAR-β is involved in the β-oxidation of fatty acid and regulates very low-density lipoprotein receptor (VLDLR) levels, influencing the development of MAFLD [44,45]. PPAR-β could upregulate genes involved in retinol esterification and downregulate inflammatory factor levels [46].

Many of vitamin A's physiological functions are mediated by retinoic acid, which activates transcriptional networks regulated by RAR and RXR. RAR is involved in regulating the expression of apolipoprotein-CIII and affects TG levels, and overexpression of hepatic RAR is thought to be associated with the development of hepatocellular carcinoma [47,48]. RXR could form obligate heterodimers with numerous other receptors, such as PPAR and RAR. RXR-selective ligands may hold potential for treating atherosclerosis and inflammatory diseases through pathways involving PPAR [49].

TCM, with its unique holistic efficacy, safety, cost-effectiveness, and history of long-term use, has emerged as an important alternative therapy for metabolic diseases, including MAFLD. HPLC revealed that the main components in WMF were chlorogenic acid, geniposide, albiflorin, paeoniflorin, and calycosin-7-*O*-glucoside. Interestingly, we found that chlorogenic acid, geniposide, albiflorin, paeoniflorin, and calycosin-7-*O*-glucoside may be associated with the regulation of PPAR-α, PPAR-β, RAR, and RXR. Current studies found that chlorogenic acid could up-regulate the expression of the PPAR-α gene in a fatty liver model [50–52]. Geniposide attenuates

chemical liver injury and increases hepatic PPAR-α expression in rats with hepatitis or alcoholic liver disease [53,54]. Albiflorin can inhibit the NF-κB signaling pathway and attenuate inflammatory response [55,56]. Paeoniflorin can up-regulate the expression of PPAR-α in the liver and attenuate hepatic steatosis in hypercholesterolemic rats [57]. These findings are consistent with the results of our study. However, our findings need to be further investigated using monomeric compounds.

5. Conclusions

Our results indicate that the pharmacodynamic material basis of WMF includes chlorogenic acid, geniposide, albiflorin, paeoniflorin, and calycosin-7-*O*-glucoside. WMF can ameliorate hepatic lipid accumulation and inflammation in MAFLD mice by regulating the PPAR signaling pathway and retinol metabolism in the liver. These results suggest that WMF may be a potential therapeutic or interventional approach in the clinical treatment of MAFLD. Still, there is a great deal of room for in-depth investigations of the safety, indications, and mechanisms of WMF.

Ethical statement

Ethics approval number: 20111119097. The animal experiments were approved by the Medical Ethics Committee of the Zhejiang University of Technology.

Data availability statement

The data associated with this study has not been deposited into any publicly available repository. The datasets used and analyzed during the current study are available from the corresponding author upon reasonable request.

Funding

This study was supported by the National Natural Science Foundation of China Nos. 81503527 and 82274134), the National Key Research and Development Plan (No. 2017YFC1702200 and 2017YFC1702202), the Key Research and Development Program of Zhejiang Province (No. 2020C04020), and the Science and Technology Department of the State Administration of Traditional Chinese Medicine Zhejiang Province Joint Project (No. GZY-ZJ-KJ-24068).

CRediT authorship contribution statement

Suhong Chen: Visualization, Validation, Supervision, Methodology, Funding acquisition. **Jiahui Huang:** Writing – review & editing, Writing – original draft, Methodology, Investigation, Formal analysis, Data curation, Conceptualization. **Yuzhen Huang:** Resources, Investigation, Data curation. **Chengliang Zhou:** Writing – original draft, Investigation, Data curation. **Ning Wang:** Methodology, Investigation. **Linnan Zhang:** Investigation. **Zehua Zhang:** Investigation. **Bo Li:** Writing – original draft, Visualization, Methodology. **Xinglishang He:** Writing – original draft. **Kungen Wang:** Visualization, Resources, Funding acquisition, Conceptualization. **Yihui Zhi:** Funding acquisition. **Guiyuan Lv:** Visualization, Supervision, Methodology, Funding acquisition. **Shuhua Shen:** Visualization, Project administration, Methodology, Funding acquisition, Conceptualization.

Declaration of competing interest

The authors declare that they have no known competing financial interests or personal relationships that could have appeared to influence the work reported in this paper.

Appendix A. Supplementary data

Supplementary data to this article can be found online at https://doi.org/10.1016/j.heliyon.2024.e33418.

References

[1] M. Eslam, P.N. Newsome, S.K. Sarin, Q.M. Anstee, G. Targher, M. Romero-Gomez, S. Zelber-Sagi, V. Wai-Sun Wong, J.F. Dufour, J.M. Schattenberg, T. Kawaguchi, M. Arrese, L. Valenti, G. Shiha, C. Tiribelli, H. Yki-Järvinen, J.G. Fan, H. Grønbæk, Y. Yilmaz, H. Cortez-Pinto, C.P. Oliveira, P. Bedossa, L. A. Adams, M.H. Zheng, Y. Fouad, W.K. Chan, N. Mendez-Sanchez, S.H. Ahn, L. Castera, E. Bugianesi, V. Ratziu, J. George, A new definition for metabolic dysfunction-associated fatty liver disease: an international expert consensus statement, J. Hepatol. 73 (1) (2020) 202–209, https://doi.org/10.1016/j.jhep.2020.03.039.

[2] M. Eslam, A.J. Sanyal, J. George, MAFLD: a consensus-Driven proposed Nomenclature for metabolic associated fatty liver disease, Gastroenterology 158 (7) (2020) 1999–2014.e1, https://doi.org/10.1053/j.gastro.2019.11.312.

[3] Z. Younossi, M. Stepanova, M. Afendy, Y. Fang, Y. Younossi, H. Mir, M. Srishord, Changes in the prevalence of the most common causes of chronic liver diseases in the United States from 1988 to 2008, Clin. Gastroenterol. Hepatol. 9 (6) (2011) 524–530, https://doi.org/10.1016/j.cgh.2011.03.020.

[4] Z. Younossi, Q.M. Anstee, M. Marietti, T. Hardy, L. Henry, M. Eslam, J. George, E. Bugianesi, Global burden of NAFLD and NASH: trends, predictions, risk factors and prevention, Nat. Rev. Gastroenterol. Hepatol. 15 (1) (2018) 11–20, https://doi.org/10.1038/nrgastro.2017.109.

[5] J. Li, B. Zou, Y.H. Yeo, Y. Feng, X. Xie, D.H. Lee, H. Fujii, Y. Wu, L.Y. Kam, F. Ji, X. Li, N. Chien, M. Wei, E. Ogawa, C. Zhao, X. Wu, C.D. Stave, L. Henry, S. Barnett, H. Takahashi, N. Furusyo, Y. Eguchi, Y.C. Hsu, T.Y. Lee, W. Ren, C. Qin, D.W. Jun, H. Toyoda, V.W.S. Wong, R. Cheung, Q. Zhu, M.H. Nguyen, Prevalence, incidence, and outcome of non-alcoholic fatty liver disease in Asia, 1999–2019: a systematic review and meta-analysis, Lancet Gastroenterol. Hepatol. 4 (5) (2019) 389–398, https://doi.org/10.1016/S2468-1253(19)30039-1.

[6] S. Man, Y. Deng, Y. Ma, J. Fu, H. Bao, C. Yu, J. Lv, H. Liu, B. Wang, L. Li, Prevalence of liver steatosis and fibrosis in the general population and various high-risk populations: a Nationwide study with 5.7 million adults in China, Gastroenterology 165 (4) (2023) 1025–1040, https://doi.org/10.1053/j.gastro.2023.05.053.

[7] F. Zhou, J. Zhou, W. Wang, X.J. Zhang, Y.X. Ji, P. Zhang, Z.G. She, L. Zhu, J. Cai, H. Li, Unexpected Rapid increase in the burden of NAFLD in China from 2008 to 2018: a systematic review and meta-analysis, Hepatology (Baltimore, Md 70 (4) (2019) 1119–1133, https://doi.org/10.1002/hep.30702.

[8] B. Gross, M. Pawlak, P. Lefebvre, B. Staels, PPARs in obesity-induced T2DM, dyslipidaemia and NAFLD, Nat. Rev. Endocrinol. 13 (1) (2017) 36–49, https://doi.org/10.1038/nrendo.2016.135.

[9] S. Francque, A. Verrijken, S. Caron, J. Prawitt, R. Paumelle, B. Derudas, P. Lefebvre, M.R. Taskinen, W. Van Hul, I. Mertens, G. Hubens, E. Van Marck, P. Michielsen, L. Van Gaal, B. Staels, PPARα gene expression correlates with severity and histological treatment response in patients with non-alcoholic steatohepatitis, J. Hepatol. 63 (1) (2015) 164–173, https://doi.org/10.1016/j.jhep.2015.02.019.

[10] L.M. Sanderson, M.V. Boekschoten, B. Desvergne, M. Müller, S. Kersten, Transcriptional profiling reveals divergent roles of PPARalpha and PPARbeta/delta in regulation of gene expression in mouse liver, Physiol. Genom. 41 (1) (2010) 42–52, https://doi.org/10.1152/physiolgenomics.00127.2009.

[11] S. Liu, B. Hatano, M. Zhao, C.C. Yen, K. Kang, S.M. Reilly, M.R. Gangl, C. Gorgun, J.A. Balschi, J.M. Ntambi, C.H. Lee, Role of peroxisome proliferator-activated receptor {delta}/{beta} in hepatic metabolic regulation, J. Biol. Chem. 286 (2) (2011) 1237–1247, https://doi.org/10.1074/jbc.M110.138115.

[12] M.R. Bono, G. Tejon, F. Flores-Santibañez, D. Fernandez, M. Rosemblatt, D. Sauma, Retinoic acid as a modulator of T cell immunity, Nutrients 8 (6) (2016), https://doi.org/10.3390/nu8060349.

[13] A. Comptour, M. Rouzaire, C. Belville, D. Bouvier, D. Gallot, L. Blanchon, V. Sapin, Nuclear retinoid receptors and pregnancy: placental transfer, functions, and pharmacological aspects, Cell. Mol. Life Sci. 73 (20) (2016) 3823–3837, https://doi.org/10.1007/s00018-016-2332-9.

[14] T.J. Cunningham, G. Duester, Mechanisms of retinoic acid signalling and its roles in organ and limb development, Nat. Rev. Mol. Cell Biol. 16 (2) (2015) 110–123, https://doi.org/10.1038/nrm3932.

[15] D.C. Berry, H. Jacobs, G. Marwarha, A. Gely-Pernot, S.M. O'Byrne, D. DeSantis, M. Klopfenstein, B. Feret, C. Dennefeld, W.S. Blaner, C.M. Croniger, M. Mark, N. Noy, N.B. Ghyselinck, The STRA6 receptor is essential for retinol-binding protein-induced insulin resistance but not for maintaining vitamin A homeostasis in tissues other than the eye, J. Biol. Chem. 288 (34) (2013) 24528–24539, https://doi.org/10.1074/jbc.M113.484014.

[16] S.E. Trasino, Y.D. Benoit, L.J. Gudas, Vitamin A deficiency causes hyperglycemia and loss of pancreatic β-cell mass, J. Biol. Chem. 290 (3) (2015) 1456–1473, https://doi.org/10.1074/jbc.M114.616763.

[17] A.A. Ashla, Y. Hoshikawa, H. Tsuchiya, K. Hashiguchi, M. Enjoji, M. Nakamuta, A. Taketomi, Y. Maehara, K. Shomori, A. Kurimasa, I. Hisatome, H. Ito, G. Shiota, Genetic analysis of expression profile involved in retinoid metabolism in non-alcoholic fatty liver disease, Hepatol. Res. 40 (6) (2010) 594–604, https://doi.org/10.1111/j.1872-034X.2010.00646.x.

[18] A. Saeed, P. Bartuzi, J. Heegsma, D. Dekker, N. Kloosterhuis, A. de Bruin, J.W. Jonker, B. van de Sluis, K.N. Faber, Impaired hepatic vitamin A metabolism in NAFLD mice leading to vitamin A accumulation in hepatocytes, Cell. Mol. Gastroenterol. Hepatol. 11 (1) (2021), https://doi.org/10.1016/j.jcmgh.2020.07.006.

[19] B. Lefebvre, Y. Benomar, A. Guédin, A. Langlois, N. Hennuyer, J. Dumont, E. Bouchaert, C. Dacquet, L. Pénicaud, L. Casteilla, F. Pattou, A. Ktorza, B. Staels, P. Lefebvre, Proteasomal degradation of retinoid X receptor alpha reprograms transcriptional activity of PPARgamma in obese mice and humans, J. Clin. Invest. 120 (5) (2010) 1454–1468, https://doi.org/10.1172/JCI38606.

[20] B. Mascrez, N.B. Ghyselinck, M. Watanabe, J.S. Annicotte, P. Chambon, J. Auwerx, M. Mark, Ligand-dependent contribution of RXRbeta to cholesterol homeostasis in Sertoli cells, EMBO Rep. 5 (3) (2004) 285–290, https://doi.org/10.1038/sj.embor.7400094.

[21] A. Michaletti, M.R. Naghavi, M. Toorchi, L. Zolla, S. Rinalducci, Metabolomics and proteomics reveal drought-stress responses of leaf tissues from spring-wheat, Sci. Rep. 8 (1) (2018) 5710, https://doi.org/10.1038/s41598-018-24012-y.

[22] X. Fu, H.C. Zhang, H. Zhang, Y. Liu, Y. Wang, Simultaneous determination of peoniflorin and albiflorin content in danggui-shaoyao-san by HPLC, Chem. Eng. (Harbin, China) 34 (1) (2020) 25–27, https://doi.org/10.16247/j.cnki.23-1171/tq.20200125.

[23] Y. Cao, G.L. Dai, Y.Q. Wang, F.R. Li, M.C. Liu, W.Z. Ju, Analysis and evaluation on atractylodes-Cyperus alcohol extract by UPLC-Q-TOF-MS/MS and HPLC, Chin. Pharmaceut. J. 58 (19) (2023) 1736–1743, https://doi.org/10.11669/cpj.2023.19.003.

[24] J.Z. Qubie, M.K. Feng, S.S. Zhang, J.L. Lan, Y.B. Hailai, Y.F. Huang, Z.M. Yang, W.B. Li, C. Chen, Y. Li, X. Liu, Y. Liu, Quality evaluation of wild Paeonia veitchii in Western Sichuan plateau based on multicomponents, Chin. Tradit. Herb. Drugs 53 (18) (2022) 5842–5850, https://doi.org/10.7501/j.issn.0253-2670.2022.18.027.

[25] Y.R. Li, L.Y. Duan, H. Wei, Y.L. Du, S.N. Zhao, H. Gao, H.F. Pan, Quality evaluation of Crataegus pinnatifida leaves by fingerprint combined with quantitative analysis of multi-components by single-marker, China Pharm. 34 (22) (2023) 2727–2733, https://doi.org/10.6039/j.issn.1001-0408.2023.22.07.

[26] W.T. Friedewald, R.I. Levy, D.S. Fredrickson, Estimation of the concentration of low-density lipoprotein cholesterol in plasma, without use of the preparative ultracentrifuge, Clin. Chem. 18 (6) (1972) 499–502. PMID: 4337382.

[27] S.S. Lei, B. Li, Y.H. Chen, X. He, Y.Z. Wang, H.H. Yu, F.C. Zhou, X. Zheng, X. Chen, N.Y. Zhang, J. Su, M.Q. Yan, G.Y. Lv, S.H. Chen, Dendrobii Officinalis, a traditional Chinese edible and officinal plant, accelerates liver recovery by regulating the gut-liver axis in NAFLD mice, J. Funct.Foods 61 (2019) 103458, https://doi.org/10.1016/j.jff.2019.103458.

[28] B. Li, S.S. Lei, J. Su, X.M. Cai, H. Xu, X. He, Y.H. Chen, H.X. Lu, H. Li, L.Q. Qian, X. Zheng, G.Y. Lv, S.H. Chen, Alcohol induces more severe fatty liver disease by influencing cholesterol metabolism, J. Evidence-based complementary altern, Méd. : eCAM 2019 (2019) 7095684, https://doi.org/10.1155/2019/7095684.

[29] D.E. Kleiner, E.M. Brunt, M. Van Natta, C. Behling, M.J. Contos, O.W. Cummings, L.D. Ferrell, Y.C. Liu, M.S. Torbenson, A. Unalp-Arida, M. Yeh, A. J. McCullough, A.J. Sanyal, Design and validation of a histological scoring system for nonalcoholic fatty liver disease, Hepatology (Baltimore, Md 41 (6) (2005) 1313–1321, https://doi.org/10.1002/hep.20701.

[30] B. Li, Z.B. Yang, S.S. Lei, J. Su, Z.W. Jin, S.H. Chen, G.Y. Lv, Combined antihypertensive effect of paeoniflorin enriched extract and metoprolol in spontaneously hypertensive rats, Phcog. Mag. 14 (53) (2018) 44–52, https://doi.org/10.4103/pm.pm_483_16.

[31] Y. Ren, G. Yu, C. Shi, L. Liu, Q. Guo, C. Han, D. Zhang, L. Zhang, B. Liu, H. Gao, J. Zeng, Y. Zhou, Y. Qiu, J. Wei, Y. Luo, F. Zhu, X. Li, Q. Wu, B. Li, W. Fu, Y. Tong, J. Meng, Y. Fang, J. Dong, Y. Feng, S. Xie, Q. Yang, H. Yang, Y. Wang, J. Zhang, H. Gu, H. Xuan, G. Zou, C. Luo, L. Huang, B. Yang, Y. Dong, J. Zhao, J. Han, X. Zhang, H. Huang, Majorbio Cloud: A one-stop, comprehensive bioinformatic platform for multiomics analyses 1 (2) (2022), https://doi.org/10.1002/imt2.12 e12.

[32] J.G. Fan, S.U. Kim, V.W.S. Wong, New trends on obesity and NAFLD in Asia, J. Hepatol. 67 (4) (2017) 862–873, https://doi.org/10.1016/j.jhep.2017.06.003.

[33] Z.M. Younossi, Non-alcoholic fatty liver disease - a global public health perspective, J. Hepatol. 70 (3) (2019) 531–544, https://doi.org/10.1016/j.jhep.2018.10.033.

[34] M. Eslam, S.K. Sarin, V.W.S. Wong, J.G. Fan, T. Kawaguchi, S.H. Ahn, M.H. Zheng, G. Shiha, Y. Yilmaz, R. Gani, S. Alam, Y.Y. Dan, J.H. Kao, S. Hamid, I.H. Cua, W.K. Chan, D. Payawal, S.S. Tan, T. Tanwandee, L.A. Adams, M. Kumar, M. Omata, J. George, The Asian Pacific Association for the Study of the Liver clinical practice guidelines for the diagnosis and management of metabolic associated fatty liver disease, Hepatol. Int. 14 (6) (2020) 889–919, https://doi.org/10.1007/s12072-020-10094-2.

[35] D.C. Hao, C.X. Liu, Deepening insights into food and medicine continuum within the context of pharmacophylogeny, Chin. Herb. Med. 15 (1) (2023) 1–2, https://doi.org/10.1016/j.chmed.2022.12.001.

[36] R.Y. Yao, C.N. He, P.G. Xiao, Food and Medicine Continuum' in the east and west: old tradition and current regulation, Chin. Herb. Med. 15 (1) (2023) 6–14, https://doi.org/10.1016/j.chmed.2022.12.002.

[37] Y.M. Chen, Q. Li, W.H. Liu, Y.H. Shi, C. Wang, Research progress on pharmacological action, clinical application and side effects of activeingredients of Salvia miltiorrhiza in the treatment of cardiovascular diseases, J. Pharm. Res. 42 (12) (2023) 1028–1034, https://doi.org/10.13506/j.cnki.jpr.2023.12.014.
[38] H.W. Li, Y.B. Nong, Q. Lin, Case repert on adverse reaction and bleeding event induced by danshen injection, Chin. J. Exp. Tradit. Med. Formulae 17 (24) (2011) 240–242, https://doi.org/10.13422/j.cnki.syfjx.2011.24.032.
[39] S.S. Lei, N.Y. Zhang, F.C. Zhou, X. He, H.Y. Wang, L.Z. Li, X. Zheng, Y.J. Dong, R. Luo, B. Li, H.Y. Jin, Q.X. Yu, G.Y. Lv, S.H. Chen, Dendrobium officinale regulates fatty acid metabolism to ameliorate liver lipid accumulation in NAFLD mice, J. Evidence-Based Complementary Altern. Med. : eCAM 2021 (2021) 6689727, https://doi.org/10.1155/2021/6689727.
[40] A.K.S. Silva, C.A. Peixoto, Role of peroxisome proliferator-activated receptors in non-alcoholic fatty liver disease inflammation, Cell. Mol. Life Sci. 75 (16) (2018) 2951–2961, https://doi.org/10.1007/s00018-018-2838-4.
[41] N. Matikainen, M.R. Taskinen, Management of dyslipidemias in the presence of the metabolic syndrome or type 2 diabetes, Curr. Cardiol. Rep. 14 (6) (2012) 721–731, https://doi.org/10.1007/s11886-012-0309-3.
[42] A. Montagner, A. Polizzi, E. Fouché, S. Ducheix, Y. Lippi, F. Lasserre, V. Barquissau, M. Régnier, C. Lukowicz, F. Benhamed, A. Iroz, J. Bertrand-Michel, T. Al Saati, P. Cano, L. Mselli-Lakhal, G. Mithieux, F. Rajas, S. Lagarrigue, T. Pineau, N. Loiseau, C. Postic, D. Langin, W. Wahli, H. Guillou, Liver PPARα is crucial for whole-body fatty acid homeostasis and is protective against NAFLD, Gut 65 (7) (2016) 1202–1214, https://doi.org/10.1136/gutjnl-2015-310798.
[43] Y. Ma, G. Lee, S.Y. Heo, Y.S. Roh, Oxidative stress is a key modulator in the development of nonalcoholic fatty liver disease, Antioxidants 11 (1) (2021), https://doi.org/10.3390/antiox11010091.
[44] M. Zarei, E. Barroso, X. Palomer, J. Dai, P. Rada, T. Quesada-López, J.C. Escolà-Gil, L. Cedó, M.R. Zali, M. Molaei, R. Dabiri, S. Vázquez, E. Pujol, Á.M. Valverde, F. Villarroya, Y. Liu, W. Wahli, M. Vázquez-Carrera, Hepatic regulation of VLDL receptor by PPARβ/δ and FGF21 modulates non-alcoholic fatty liver disease, Mol. Metabol. 8 (2018) 117–131, https://doi.org/10.1016/j.molmet.2017.12.008.
[45] A. Wolf Greenstein, N. Majumdar, P. Yang, P.V. Subbaiah, R.D. Kineman, J. Cordoba-Chacon, Hepatocyte-specific, PPARγ-regulated mechanisms to promote steatosis in adult mice, J. Endocrinol. 232 (1) (2017) 107–121, https://doi.org/10.1530/JOE-16-0447.
[46] W. Shan, P.S. Palkar, I.A. Murray, E.I. McDevitt, M.J. Kennett, B.H. Kang, H.C. Isom, G.H. Perdew, F.J. Gonzalez, J.M. Peters, Ligand activation of peroxisome proliferator-activated receptor beta/delta (PPARbeta/delta) attenuates carbon tetrachloride hepatotoxicity by downregulating proinflammatory gene expression, Toxicol. Sci. 105 (2) (2008) 418–428, https://doi.org/10.1093/toxsci/kfn142.
[47] S.J. Lee, M. Mahankali, A. Bitar, H. Zou, E. Chao, H. Nguyen, J. Gonzalez, D. Caballero, M. Hull, D. Wang, P.G. Schultz, W. Shen, A novel role for RARα agonists as apolipoprotein CIII inhibitors identified from high throughput screening, Sci. Rep. 7 (1) (2017) 5824, https://doi.org/10.1038/s41598-017-05163-w.
[48] A. Yanagitani, S. Yamada, S. Yasui, T. Shimomura, R. Murai, Y. Murawaki, K. Hashiguchi, T. Kanbe, T. Saeki, M. Ichiba, Y. Tanabe, Y. Yoshida, S.I. Morino, A. Kurimasa, N. Usuda, H. Yamazaki, T. Kunisada, H. Ito, Y. Murawaki, G. Shiota, Retinoic acid receptor alpha dominant negative form causes steatohepatitis and liver tumors in transgenic mice, Hepatology (Baltimore, Md 40 (2) (2004) 366–375, https://doi.org/10.1002/hep.20335.
[49] A.I. Shulman, D.J. Mangelsdorf, Retinoid x receptor heterodimers in the metabolic syndrome, N. Engl. J. Med. 353 (6) (2005) 604–615, https://doi.org/10.1056/NEJMra043590.
[50] M.B. Sanchez, E. Miranda-Perez, J.C.G. Verjan, M. de Los Angeles Fortis Barrera, J. Perez-Ramos, F.J. Alarcon-Aguilar, Potential of the chlorogenic acid as multitarget agent: insulin-secretagogue and PPAR α/γ dual agonist, Biomed. Pharmacother. 94 (2017) 169–175, https://doi.org/10.1016/j.biopha.2017.07.086.
[51] C.W. Wan, C.N.Y. Wong, W.K. Pin, M.H.Y. Wong, C.Y. Kwok, R.Y.K. Chan, P.H.F. Yu, S.W. Chan, Chlorogenic acid exhibits cholesterol lowering and fatty liver attenuating properties by up-regulating the gene expression of PPAR-α in hypercholesterolemic rats induced with a high-cholesterol diet, Phytother Res. 27 (4) (2013) 545–551, https://doi.org/10.1002/ptr.4751.
[52] A.S. Cho, S.M. Jeon, M.J. Kim, J. Yeo, K.I. Seo, M.S. Choi, M.K. Lee, Chlorogenic acid exhibits anti-obesity property and improves lipid metabolism in high-fat diet-induced-obese mice, Food Chem. Toxicol. 48 (3) (2010) 937–943, https://doi.org/10.1016/j.fct.2010.01.003.
[53] C. Li, K. Zhang, X. Jin, X. Gao, J. Lv, J. Shen, X. Gao, H. Zhang, J. Sun, A transcriptomics and network pharmacology approach to elucidate the mechanism of action of geniposide on carbon tetrachloride-induced liver injury in rats, Int. Immunopharm. 120 (2023) 110391, https://doi.org/10.1016/j.intimp.2023.110391.
[54] T. Ma, C. Huang, G. Zong, D. Zha, X. Meng, J. Li, W. Tang, Hepatoprotective effects of geniposide in a rat model of nonalcoholic steatohepatitis, J. Pharm. Pharmacol. 63 (4) (2011) 587–593, https://doi.org/10.1111/j.2042-7158.2011.01256.x.
[55] R. Yang, Y. Yang, Albiflorin attenuates high glucose-induced endothelial apoptosis via suppressing PARP1/NF-κB signaling pathway, Inflamm. Res. 72 (1) (2023) 159–169, https://doi.org/10.1007/s00011-022-01666-z.
[56] X. Wang, L. Su, J. Tan, T. Ding, Y. Yue, Albiflorin alleviates DSS-induced ulcerative colitis in mice by reducing inflammation and oxidative stress, Iran, J. Basic Med. Sci. 26 (1) (2023) 48–56, https://doi.org/10.22038/IJBMS.2022.66678.14624.
[57] H. Hu, Q. Zhu, J. Su, Y. Wu, Y. Zhu, Y. Wang, H. Fang, M. Pang, B. Li, S. Chen, G. Lv, Effects of an enriched extract of paeoniflorin, a monoterpene glycoside used in Chinese herbal medicine, on cholesterol metabolism in a hyperlipidemic rat model, Med. Sci. Mon. Int. Med. J. Exp. Clin. Res. 23 (2017) 3412–3427, https://doi.org/10.12659/msm.905544.